Rheological Monitoring of Polyacrylamide Gelation: Importance of Cross-Link Density and Temperature

Damien Calvet,[†] Joyce Y. Wong,[‡] and Suzanne Giasson*[,†]

Département de Chimie et Faculté de Pharmacie, Université de Montréal, C.P. 6128, succursale Centre-Ville, Montréal QC, Canada H3C 3J7, and Department of Biomedical Engineering, Boston University, 44 Cummington Street, Boston, Massachusetts 02215

Received May 11, 2004

ABSTRACT: Dynamic shear oscillation measurements at small strains are used to characterize the polymerization process in situ and the viscoelastic properties of cross-linked polyacrylamide hydrogels. Hydrogels are synthesized by free-radical redox polymerization of acrylamide (8 wt %) for different concentrations of cross-linker, *N*,*N*′-methylenebis(acrylamide) (BIS), at different temperatures. Both elastic modulus G' and viscous modulus G'' are measured in real time during the gelation which takes place directly between parallel rheometer plates. The elastic modulus G' remains constant with frequency, $G'(\omega) \approx cte$, and is significantly larger than $G''(\omega)$, characteristic of a well-developed cross-linked polymer network. Temperature scanning of the elastic modulus shows that $G'(T)$ is a linear relationship with a proportionality value that depends on the polymerization temperature T_{pol}. This observation is in agreement with the classical theory of rubberlike elasticity, i.e., $G' = n_e RT$ where n_e is the active network links density. The results confirm that the final G' and G'' are sensitive to the cross-linker concentration as well as the polymerization temperature. Moreover, G' follows a linear progression over a large range of BIS concentration. For a given acrylamide monomer concentration, there exists an optimal bis-(acrylamide) cross-linker concentration and an optimal polymerization temperature which give rise to an "ideal" hydrogel, i.e., exhibiting a maximal elasticity.

1. Introduction

For the past three decades, polyacrylamide cross-linked hydrogels (PAAm) have been widely studied. The intrinsic structure of these three-dimensional polymeric networks generates very interesting material properties that have been exploited in a number of important applications. For example, high swelling capacity[1] is very useful for water retention applications; variable mesh size porosity[2,3] is ideal in electrophoresis for separating protein and DNA samples and also in model drug delivery systems[4] to study controlled drug release profiles; and more recently, easy modulation of hydrogel stiffness, by tuning the monomer/cross-linker ratio, has shown that PAAm is an excellent model substrate for fundamental studies (e.g., cell motility studies[5,6]) to advance the development of biomaterials for tissue engineering[7] applications. Therefore, it is highly desirable to elucidate the effects of PAAm polymerization conditions on structure−property relationships to optimize functional performance. Because cross-linked hydrogels mainly develop a rubberlike rheological behavior,[8] mechanical characterizations are mainly performed by measuring Young's modulus[9] or swelling ratio.[10,11] Recently, Durmaz et al.[12] demonstrated large local variations of the Young's modulus in macroscopic gel samples, indicating the presence of macrosized inhomogeneities in the gel structure, resulting from sedimentation before the sol−gel transition. However, measurements obtained from Young's modulus or swelling ratio experiments do not reveal the kinetics of the reaction and therefore are not useful in determining the optimal polymerization conditions for hydrogels with desired properties. In contrast, rheological monitoring is attractive because it can be carried out in situ, i.e., during the polymerization process, and therefore can be used to directly test the importance of parameters such as cross-link density and polymerization temperature on properties such as elasticity.

Kinetics of in situ gelation and resulting rheological properties of different species of gels can be easily studied using oscillatory deformation tests.[13−16] The complex shear modulus (G^*) measured can be resolved into its real component (G') and imaginary component (G''):

$$G^* = G' + iG'' \tag{1}$$

The elastic (or storage) modulus G' is a measure of the reversibly elastic storage deformation energy, whereas the viscous (or loss) modulus G'' represents a measure of the irreversible energy dissipated during flow. Cross-linked hydrogels have a specific behavior which corresponds to a dominant and non-frequency-dependent elastic modulus, $G'(\omega) = cte$.[8,17] For permanently cross-linked gels, the equilibrium shear elasticity can be predicted by the theory of rubber elasticity first developed by Flory,[18,19] which can be expressed by the following equation:[20,21]

$$G_e = (1 - 2/f)\nu_e RT\frac{\langle r^2\rangle}{\langle r_0^2\rangle} \tag{2}$$

which allows the number of effective chains per unit volume ν_e to be estimated (in mol m^{-3}). R is the universal gas constant (8.314 J mol^{-1} K^{-1}), T is the temperature, $\langle r^2\rangle$ represents the average square end-to-end distance in the swelled state, and $\langle r_0^2\rangle$ is the value of $\langle r^2\rangle$ at the end of the gelation process. For freshly prepared and unswelled hydrogels $\langle r^2\rangle = \langle r_0^2\rangle$.

[†] Université de Montréal.
[‡] Boston University.
* Corresponding author: Tel +1-514-343-5614; fax +1-514-343-7586; e-mail suzanne.giasson@umontreal.ca.

10.1021/ma049072r CCC: $27.50
Published on Web 09/03/2004

The functionality f is the number of strands linked to a cross-linker. The density ν_e is related to the density of effective junctions n_e (in mol m^{-3}) using the following equality:[21]

$$\nu_e = \left(\frac{f}{2}\right) n_e \tag{3}$$

From eqs 2 and 3, the elastic modulus is expected to be proportional to n_e at constant temperature, but as well as proportional to T at constant n_e. The concentration of effective network junction n_e is usually different that the one expected by the cross-linker concentration: several unreacted BIS molecules can cluster together and contribute to one elastically effective cross-link, or dangling or cyclic chains can form that are not effective strands in the hydrogel network.[20] Because of the dominant elastic character, the viscous modulus G'' is generally on the order of 0.1%−5% of G' values and can be neglected.[21] The mechanical behavior of rubber-like hydrogels,[12] their swelling ratio,[4,11] and porosity[2] are mainly dependent on the architecture of the polymer network.[8] Architecture specifications appear during the polymerization process and depend on the monomer concentration,[22] cross-linking density and nature,[1,12,23] and the polymerization conditions such as temperature,[11] solvent,[24−26] or shear rate.[27] For hydrogels composed of acrylamide (AAm) and *N*,*N*′-methylenebis-(acrylamide) (or bis(acrylamide) or BIS), the usual terminology of *%T* refers to the total mass of both monomer AAm, m_{AAm}, and the cross-linker BIS, m_{BIS}, as a percentage of the total volume of the solution, V_{sol}, (w/v):[28]

$$\%T = \frac{m_{AAm} + m_{BIS}\,(g)}{V_{sol}\,(mL)} \times 100 \tag{4}$$

The term *%C* refers to the relative concentration of the cross-linker BIS (w/w) as a fraction of *%T*:

$$\%C = \frac{m_{BIS}\,(g)}{m_{AAm} + m_{BIS}\,(g)} \times 100 \tag{5}$$

Twenty five years ago, Weiss and Sildeberg[16] determined both G' and G'' moduli using Couette geometry to show that the hydrogel structure consists of spherical cores of high density (with radii about 10 nm or so with $4 \le \%T \le 10$ and $1 \le \%C \le 8$) surrounded by a much more dilute phase. Recently, numerous improvements in rheology techniques have led to better control in measuring the stress, the strain, and also the temperature, making possible the monitoring of the gelation process in situ. More recently, Grattoni et al. [14] measured G' and G'' during the gelation process of PAAm cross-linked with chromium acetate cross-linker (Cr^{3+}), using a Couette geometry at low-amplitude strain, constant-frequency oscillatory shear, and at 70 °C. They showed that the final elastic and the viscous moduli increase with polymer concentration according to a power-law relationship. Kulicke and Nottelmann[21] used plate−plate geometry to measure elastic modulus of PAAm hydrogel cross-linked using BIS. In that study, the hydrogels were first synthesized, and so no rheological monitoring of the gelation process was performed. They observed a general behavior of G' as a function of *%C* corresponding to an increase of G', reaching a maximum for $\%C \approx 5$, where the hydrogel is considered as an "ideal" gel.[1,9,21] Trompette et al.[29] confirmed that the complex modulus of cross-linked PAAm increases with BIS concentration for a given monomer concentration but also increases as the concentration of acrylamide monomer increases for a given BIS concentration.

PAAm hydrogels have been widely studied using other techniques in order to investigate its mechanical behavior as well as its network structure (mesh size). From high-resolution ^{1}H NMR analysis of the gelation process, Baselga et al.[30] suggested that there are three different steps in the cross-linking copolymerization of AAm and BIS: pregel reaction, gelation, and postgel reactions. Pregel reaction leads to the formation of soluble particles (or microgels) that are richer in BIS molecules due to their high reactivity with the growing polymer chains compared to AAm molecules. During gelation, the pregel particles are linked by polymerized AAm chains that are poorer in BIS than the microgels. The postgel reactions would correspond to the formation of dangling AAm chains since most of BIS molecules have previously been consumed.[30] More recently, Pekcan and Kara[3,31] confirmed the existence of "frozen blob clusters" in the gel using photon transmission technique during the swelling of PAAm hydrogel. While differences in the kinetics of these different steps have been observed, it is not clear what the impact is on the mechanical properties of the hydrogel. For example, one would expect polymerization temperature to have an effect on different molecules' reactivity.

Surprisingly, there is only scanty literature on the relationship between hydrogel properties and temperature of polymerization (T_{pol}).[24−26] Gelfi and Righetti[24] have shown that PAAm hydrogels exhibit a transition between a milky and clear appearance as polymerization temperature increases. Furthermore, the authors have demonstrated the importance of T_{pol} on the polymerization kinetics. It is well-known that the higher the T_{pol}, the faster the gelation.[24,25] Takata et al.[25] and, more recently, Peckan and Kara[11] demonstrated that, depending on the polymerization temperature, the microscopic structures of PAAm hydrogels change; i.e., gels prepared at high temperature have compact internal structures.

According to Flory's gelation theory,[18] the polymerization process is governed by the monomers reactivity, the cross-linker functionality, and the monomers concentrations. If the functionality and monomer concentrations are fixed, the reactivity can be modulated by changing the temperature. The aim of this paper is to examine the importance of the cross-linker concentration, *%C*, and the polymerization temperature, T_{pol}, on the final rheological properties of the hydrogel. The rheological properties of hydrogel are determined throughout the entire cross-linking process using parallel-plate geometry. To our knowledge, no rheological investigation has yet been conducted for AAm/BIS cross-linked hydrogels using in situ rheological monitoring of the gelation process under controlled polymerization temperatures.

2. Materials and Experimental Methods

2.1. Materials, Synthesis, and Polymer Nomenclature. The cross-linked polyacrylamide hydrogels were synthesized according to the procedure used for electrophoresis.[32] Acrylamide aqueous solution (AAm, the monomer) (40 wt %), *N*,*N*′-methylenebis(acrylamide) (BIS, the cross-linker) aqueous solution (2 wt %), *N*,*N*,*N*′,*N*′-tetramethylethylenediamine

Table 1. Volume of 2% (w/w) of *N,N′*-Methylenebis(acrylamide) Solution Used in the Synthesis of Cross-Linked PAAm Hydrogels

name	vol BIS (mL)	%*C*	[BIS][a] (mol m^{-3})	Am/BIS ratio
PA20-050	0.2	0.50	2.60	433.3
PA20-100	0.4	1.00	5.19	216.7
PA20-184	0.75	1.84	9.74	115.6
PA20-315	1.3	3.15	16.88	57.8
PA20-361	1.5	3.61	19.48	66.7
PA20-476	2	4.76	25.97	43.3
PA20-521	2.2	5.21	28.57	39.4
PA20-566	2.4	5.66	31.17	36.1
PA20-698	3	6.98	38.96	28.9

[a] The BIS relative concentration *%C* is calculated using eq 5.

(TEMED, the catalyst), and ammonium persulfate (APS, the initiator) were purchased from BioRad and were used as received. Free radical polymerization of acrylamide initiated with TEMED/APS is characterized by redox and can be performed at room temperature.[25] Because oxygen inhibits the reaction, exposure of the monomer solution to air must be minimized.

The reactive solution was prepared by mixing 2 mL of AAm, 15 μL of TEMED, different amounts of BIS solutions (Table 1), and distilled water to attain a final volume of 10 mL. Finally, 50 μL of freshly prepared APS solution (10 wt %) was added just before the measurements because of fast degradation of APS in water at room temperature.

To differentiate the various hydrogel syntheses, a simple nomenclature to specify the polymerization temperature T_{pol} and the value of *%C* (eq 5) is used. For example, PA20-184 corresponds to polyacrylamide synthesized at 20 °C with *%C* = 1.84 (Table 1).

For synthesis of the un-cross-linked PAAm, the monomer solution is the same as described for cross-linked hydrogel synthesis, except no bis(acrylamide) is added.

2.2. Rheological Measurements. Rheological measurements of the PAAm gels were carried out using an AR 2000 rheometer (TA Instruments, Newcastle, DE) equipped with a Peltier device for temperature control. Parallel-plate geometry was used. The upper plate is made of stainless steel with a 10 mm radius. The lower plate is the Teflon Pelletier surface. During all rheological experiments, a solvent trap was used to minimize evaporation. Initiator was added to the reactive solution, 0.16 mL was poured on the lower plate, and then the upper plate was set at the desired separation distance (500 μm). This preparation step lasts about 30 s. An angular frequency of $\omega = 1$ rad s^{-1} and deformation of $\gamma^0 = 0.01$ were selected to ensure a linear regime of oscillatory deformation. The macrostructure of the gel was not ruptured during the different rheological experiments. Because shear rate can influence the polymerization process,[27] constant ω and γ^0 values were used for all experiments. For constant oscillation frequency, elastic and viscous moduli are defined as[17]

$$G' = (\sigma^0/\gamma^0)\cos\delta \quad \text{and} \quad G'' = (\sigma^0/\gamma^0)\sin\delta \qquad (6)$$

where δ is the phase shift between the strain and stress waves. During the gelation process, elastic modulus G' and viscous modulus G'' were recorded every minute for $T_{pol} \geq 30$ °C or every 2 min for $T_{pol} < 30$ °C.

In general, it is quite difficult to obtain reproducible rheological data for hydrogels below the standard 10% error due to the gel degradation by hydrolysis of the amide function[25,33] or to a potential swelling or deswelling process before the rheological test. These sources of error were minimized by rheological monitoring of PAAm polymerization which allows the elastic properties of freshly prepared gels to be determined immediately after the gelation process.

Once the polymerization was completed (i.e., at constant G' and G''), dynamic frequency sweep tests were recorded in a constant strain mode ($\gamma^0 = 0.01$) maintained over the frequency range of 0.1−100 rad s^{-1} at 20 °C. The temperature dependence of the elastic modulus of the different polymerized hydrogels was determined using constant oscillatory deformation ($\gamma^0 = 0.01$ and $\omega = 1$ rad s^{-1}) for temperature ranging from 5 to 42.5 °C, allowing 5 min of equilibrium between each measurements. Because the hydrogel was quite thin (500 μm), the solution temperature quickly reached equilibrium.

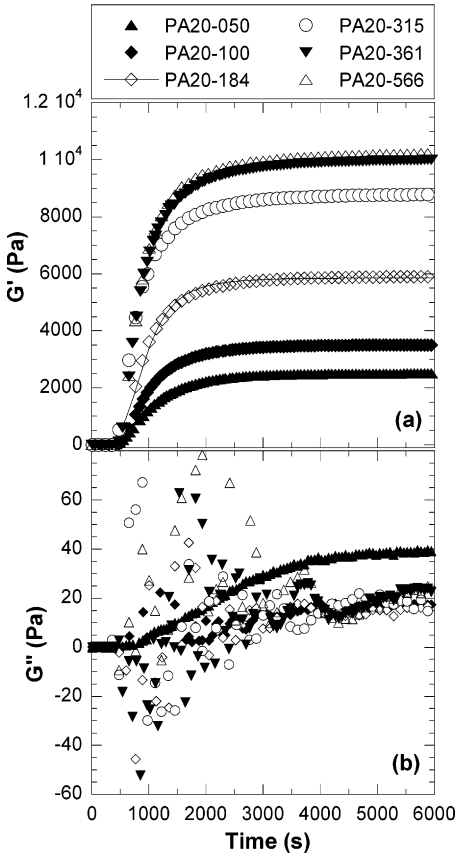

Figure 1. Variations of (a) elastic moduli G' and (b) viscous moduli G'' during the polymerization for different BIS cross-linker concentrations (*%C*). All polymerizations were performed at 20 °C under dynamic oscillations using $\omega = 1$ rad s^{-1} and $\gamma^0 = 0.01$. The solid line in (a) represents a fit curve example using the modified Hill equation (eq 7).

For the high viscoelastic properties of un-cross-linked PAAm, an acrylic cone with a 60 mm diameter, an angle of 2°, and a truncature of 68 μm were used. A 2 mL aliquot of the pregel solution was deposited on the lower Teflon plate maintained at a fixed temperature ($T_{pol} = 5$, 10, 20 or 30 °C), and then the cone was set at the desired separation distance (68 μm). During the polymerization process, oscillatory deformations were applied using a constant stress of 1 Pa and a constant frequency of 1 rad s^{-1}. Flow viscosity $\eta(\dot{\gamma})$ was measured at 20 °C with $0.01 \leq \dot{\gamma} \leq 100$ s^{-1}.

3. Results and Discussion

For all studies, average and standard deviations were calculated from a minimum of three different measurements

3.1. Influence of Cross-Linker Concentration (*%C*). Figure 1 illustrates the elastic and viscous moduli recorded during hydrogel polymerization for different cross-linker BIS concentrations at constant temperature of 20 °C. The different values of *%C* (Table 1) correspond to a Acrylamide/BIS molar ratio ranging from 28.9 to 433.3. After a certain induction period, i.e., period during which the elastic moduli are negligible, the elastic modulus $G'(t)$ increases monotonically and reaches a plateau value (Figure 1a). At low BIS concentration (PA20-050), the viscous modulus $G''(t)$ exhibits a be-

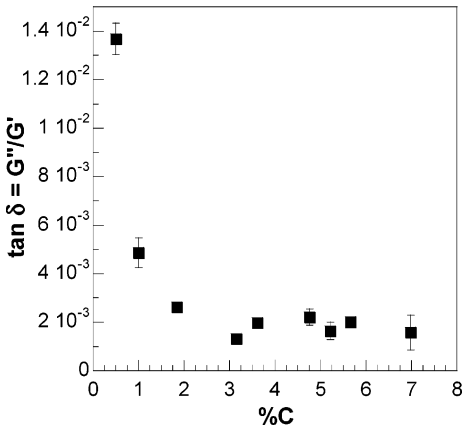

Figure 2. tan $\delta = G''/G'$ as a function of *%C*. G' are obtained from the fit (eq 7), and G'' are the steady-state regime observed in Figure 1b at $T = 20$ °C.

havior similar to $G'(t)$ (Figure 1b). The final value of G'' is ca. 40 Pa, which is 65 times smaller than G'. For higher *%C* (PA20-100 to PA20-698), $G''(t)$ values oscillate around zero at the beginning of the polymerization process and then stabilize to a constant value. The random variation G'' is due to the sensitivity limit of the rheometer in the determination of δ that oscillates around zero (cf. eq 6 and Figure 1b). The polymerization process is assumed to be completed when $G'(t)$ and $G''(t)$ reach a plateau value with time, and then tan $\delta = G''/G'$ can be determined (Figure 2). The plateau values of G'' are about 0.21 ± 0.05% of G'. Such small values of G'' can be neglected compared with the elastic modulus.[21]

From the $G'(t)$ plot (Figure 1), three different periods in the gelation process can be defined: (1) an initiation period where G' remains close to zero, (2) a sol−gel transition period where G' increases dramatically, and (3) a plateau regime where G' slightly increases to reach the final equilibrium value. The experimental data $G'(t)$ were fitted to a modified Hill equation:[34,35]

$$G'(t) = G'\frac{t^n}{t^n + \theta^n} \tag{7}$$

G' (in Pa) corresponds to the final steady-state elastic modulus. The half-gelation time θ is the time (in seconds) for which $G(\theta) = G'/2$. Finally, n is a coefficient relative to the asymptotic slope P (in Pa s^{-1}) at the half-gelation time θ with

$$P = \frac{nG'}{4\theta} \tag{8}$$

Equation 8 can be used to quantitatively characterize the sol−gel transition kinetics. For clarity, only one fitting curve is plotted in Figure 1a for the hydrogel PA20-184 (solid line, open diamonds). The values of G', n, and θ extracted from the fits for different cross-linker concentration are plotted in function of *%C* in Figure 3. For low *%C* (≤3.61), G'(*%C*) follows a linear relationship but reaches a plateau at 11113 ± 138 Pa (*%C* = 4.21). An increase in G'(*%C*) up to a maximum value followed by a plateau or a decrease is a general behavior previously reported.[16,21−23] However, only from the results reported by Weiss and Silberger,[16] one can distinguish a linear relationship between G' and low *%C* at different *%T*. The results shown in Figure 3 are also in agreement with previous studies showing a maximum

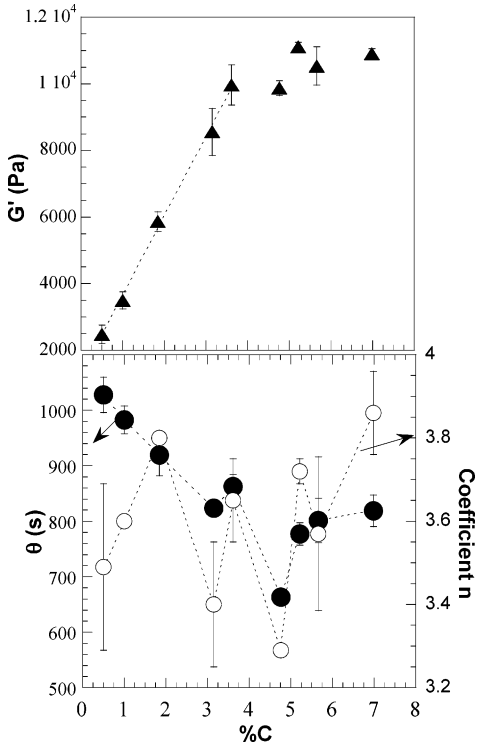

Figure 3. (a) Steady state G' obtained from the fit (eq 7) as a function of *%C*. Dotted line represents a linear fit for *%C* ≤ 3.61: $G'(\%C) = 1261 + 2382(\%C)$ with $R = 0.996$. (b) Half-gelation time θ (closed circles, left scale) and coefficient n (open circles, right scale) with *%C*.

elasticity at *%C* ≈ 5, which is generally explained by the presence of heterogeneities in the gel.[16,21,36] As shown in Figure 3b, half-gelation time θ first slightly decreases with increase in *%C* (from about 1000 to 800 s) but stabilizes for *%C* ≥ 3.6. Coefficient n oscillates around 3.6. The sol−gel transition kinetics increases as *%C* increases up to *%C* = 3.61. For larger *%C* values, the cross-linker concentration does not influence the gelation kinetics (Figure 3a).

Once polymerization is achieved, i.e., when $G'(t)$ and $G''(t)$ reached a constant value (Figure 1a), dynamic oscillatory tests in frequency were performed up and down between 0.1 and 100 rad s^{-1} (Figure 4a). The reproducibility of $G'(\omega)$ data between the up and down tests confirms that the polymerization process reached completion. Figure 4a shows $G'(\omega)$ and $G''(\omega)$ for PA20-050 and PA20-566. For the soft hydrogel PA20-050, $G'(\omega)$ increase from 2468 Pa ($\omega = 1$ rad s^{-1}) to 2780 Pa ($\omega = 100$ rad s^{-1}), corresponding to a gain in G' of 12.6%. In contrast, for the stiff hydrogel PA20-566, $G'(\omega)$ is constant around 10 350 Pa with a standard deviation of 36 Pa. For the soft hydrogel PA20-050, $G''(\omega)$ exhibits a power law behavior (cf. Figure 4a). For a stiffer hydrogel such as PA20-566, $G''(\omega)$ exhibits random behavior around a value of 26 ± 16 Pa, which is negligible compared to $G'(\omega)$. The stability and the relative large value of $G'(\omega)$ compared to $G''(\omega)$ over a range of at least three decades is a characteristic feature of a cross-linked hydrogel. This stability also suggests that the permanent chemical cross-links are not destroyed by the increasing frequency at constant strain γ^0. $\gamma^0 = 0.01$ is within the linearity domain. Indeed, G' was measured as a function of increasing strain amplitude γ^0 (Figure 4b). G' remains constant for low strains ($\gamma^0 > 1$ for PA20-050, $\gamma^0 \leq 1$ for PA20-315, and $\gamma^0 \leq 0.2$

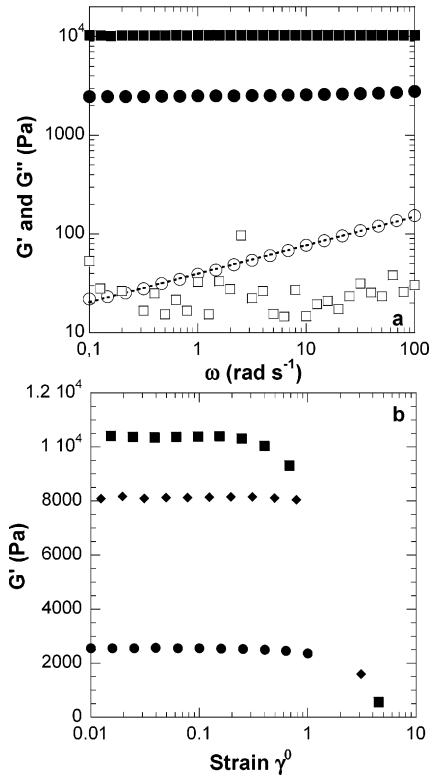

Figure 4. (a) $G'(\omega)$ (closed symbols) and $G''(\omega)$ (open symbols) as functions of frequency ω measured for PA20-566 (squares) and PA20-050 (circles) using $\gamma^0 = 0.01$ and $T = 20$ °C. Dotted line correspond to the exponential fit of $G''(\omega)$: $G''(\omega) = 39.7\omega^{0.28}$ with $R = 0.999$. (b) $G'(\omega)$ as a function of strain amplitude γ^0 for PA20-050 (circles), PA20-315 (diamonds), and PA20-566 (squares) using $\omega = 10$ rad s^{-1} and $T = 20$ °C.

for PA20-566). The linearity domain decreases as the elasticity of the hydrogel increases.

For the BIS cross-linker used in the PAAm hydrogels synthesis, the functionality f is theoretically equal to 4 because one cross-linker molecule can potentially be linked with four linear strands. Furthermore, the equilibrium shear elastic modulus G_e in the theory of rubber elasticity (eq 2) corresponds to the frequency-independent elastic modulus G' (plateau modulus). Combining eqs 2 and 3 with $f = 4$, G' can then be expressed as

$$G' = n_e RT \tag{9}$$

This equation means that, for a constant value of n_e, an increase in the measurement temperature T must theoretically lead to a proportional increase in G'. The hydrogel is not in contact with external solvent and is assumed to remain in its primitive swollen state throughout the experiment ($\langle r_0^2 \rangle = \langle r^2 \rangle$ in eq 2), leading to a constant network junction density n_e. Values of G' were measured as a function of different values of T, and results are presented in Figure 5. No hysteresis between the heating and cooling mode was observed, and $G'(T)$ is directly proportional to T as expressed in eq 9. The density of active junctions n_e (in mol m^{-3}) are then extracted from the experimental data ($G'(T)$, Figure 5 using eq 9). Figure 6 represents n_e as a function of $\%C$, showing that $n_e(\%C)$ exhibits the same general behavior that $G'(\%C)$ (Figure 3), with an linear increase followed by a plateau The values of n_e obtained account for 43% of the theoretical cross-link densities for $\%C = 0.5$ and only 18% for $\%C = 5.66$ (calculated assuming that each BIS molecule forms one cross-link), meaning that the

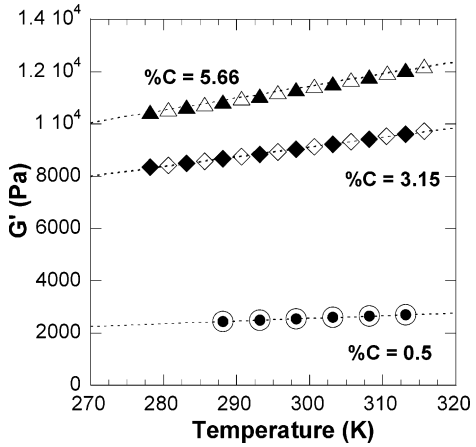

Figure 5. Evolution of the elastic modulus G' ($\omega = 1$ rad s^{-1}, $\gamma = 0.01$) of PA20-050 (circles), PA20-315 (diamonds), and PA20-566 (triangles) as a function of temperature (with an equilibrium time of 5 min before each measurements). Closed symbols represent tests performed in heating mode, and open symbol represents the cooling mode. Solid lines represent linear fitting.

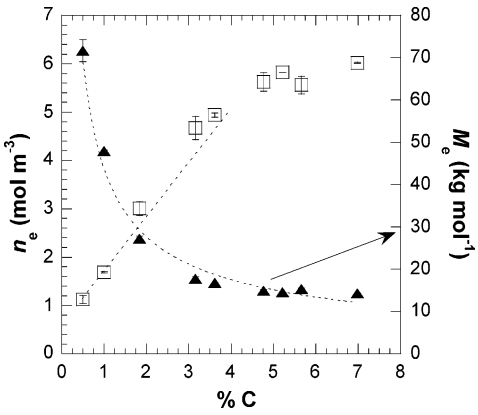

Figure 6. Number of networks junctions n_e (open squares, left scale) and strands molecular weights M_e (closed triangles, right scale) as a function of $\%C$. n_e values are estimated from fitted curves (Figure 5) using eq 9. For $\%C \leq 3.61$, n_e is a linear function of $\%C$: $n_e = 0.51 + 1.28$ ($\%C$) with $R = 0.999$. M_e is calculated using eq 10. Dotted line present power-law relationship between M_e and $\%C$.

cross-linker molecules are less efficient in the formation of network junction as $\%C$ increases. This can be explained by the fact that (1) some BIS molecules do not react during the gelation process, (2) more than two cross-linker molecules participate to the formation of just one cluster which correspond in fact at only one active rheological junction in the network, and (3) some BIS molecules participate in the formation of dangling or cyclic chains which are not elastically active.

Knowing the numbers of active junctions n_e, the strand molecular weight M_e (in kg mol^{-1}) corresponding to one polymer chain linking two junctions can be estimated using the following relation:[21]

$$M_e = \frac{[\mathrm{AAm}]}{n_e} \tag{10}$$

with [AAm] being the total acrylamide monomer concentration in kg m^{-3}. M_e as a function of $\%C$ is plotted in Figure 6. When increasing the cross-linker concentration, the strand mesh size decreases down to a minimum value of 19 kg mol^{-1} for $\%C \geq 3.15$; i.e., the porosity of the gel decreases with increasing $\%C$.

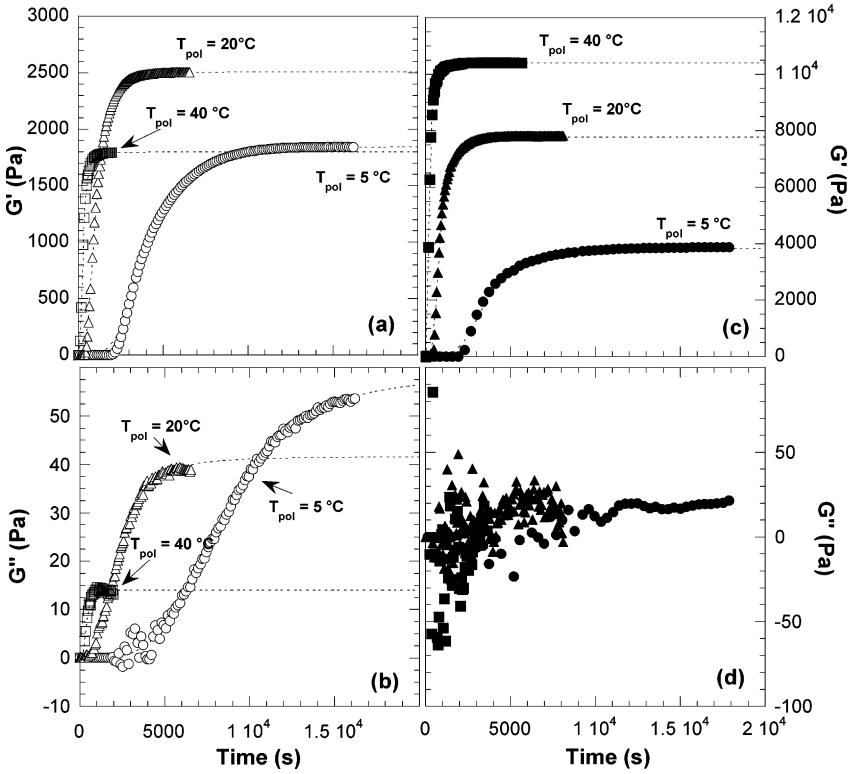

Figure 7. Evolution of the elastic G' and G'' with time (with $\omega = 1$ rad s^{-1} and $\gamma^0 = 0.01$) for three different polymerization temperatures: $T_{pol} = 5$ °C (circles), 20 °C (triangles), and 40 °C (squares); for (a) and (b) $\%C = 0.5$ and for (c) and (d) $\%C = 3.15$. Dotted lines represent the fitting curves according to eq 7.

It is known that the reactivity of living radicals is relatively higher with BIS than with AAm,[9] leading to an initial formation of free microgel particles (cross-linked clusters) in solution[36,37] during the initiating period. If there is no bridging between these microgels, the solution does not exhibit any apparent elasticity because it cannot store energy at equilibrium. The time at which G' shows a yield point (Figure 1) corresponds to the emergence of "interjunction" links, the beginning of the sol−gel transition period. The variation of G' with T allows neither the nature (size, shape) of these junctions nor the microgel structure to be determined. The irregularities usually observed in the hydrogel structure might arise from the formation of dangling chains due to a termination of the growing polymer chain prior to cross-linking, the presence of polymer rings which do not participate in the network, and the presence of sol fraction (i.e., molecular species that are not attached to the network).[38] Permanent entanglements, formed between the linear chains and trapped in the course of the cross-linking process, represent active junctions in the polymer network that increase the change of entropy with deformation and contribute to the elasticity of the hydrogel as the chemical cross-linkers themselves. In eq 9, the number n_e is in fact the sum of the number of chemical junctions and permanent entanglements.[38] For stiff hydrogels, the elasticity does not depend on the shear frequency, but for the softer hydrogels, $G'(\omega)$ slightly increases with increasing frequency, which suggests the formation of nonpermanent junctions (e.g., hydrogen bonds or perhaps reversible entanglements) between polymeric chains. Finally, a higher mobility of higher molecular weight strands (M_e) might allow permanent entanglements to be activated as the chains are stretched under increasing shear rate. The increase in $G''(\omega)$, significant only for the soft hydrogel PA20-050 (Figure 4), might correspond to an increase in the trapped effective solution viscosity in the highest network tightness. At higher cross-linker concentration, the polymer chains are shorter (Figure 6), and elastic or viscous moduli are not modulated by the rising shear rate, suggesting that the creation of new junctions is not probable.

3.2. Influence of the Polymerization Temperature. The temperature of polymerization influences the reactivity of the different molecules present in solution (Arrhenius law)[39] and therefore affects the rates of dissociation of the initiator (ammonium persulfate) into free radicals,[40] the polymerization propagation between bis(acrylamide) and acrylamide, and the acrylamide coupling and ending reaction kinetics by radicals coupling reaction. To investigate the role of each of the reactive molecules during polymerization and in particular the initiator activity, the effect of the polymerization temperature was determined for PAAm hydrogels with $\%C = 0.5$, 3.15, and 5.66, for temperatures ranging from 5 to 60 °C. The evolution of G' and G'' as a function of time, $G'(t)$ and $G''(t)$, for $T_{pol} = 5$, 20, and 40 °C are reported in Figure 7a,b for $\%C = 0.5$ and for $\%C = 3.15$ in Figure 7c,d. The steady-state elastic moduli G' are strongly dependent on T_{pol}. As observed previously, steady-state viscous moduli G'' remain significantly smaller than G'. Instabilities in G'' measurements are observed for $\%C > 0.5$ (Figure 7d). The induction period decreases as T_{pol} increases (Figure 7a,c). More precisely, at $T_{pol} = 5$ °C the induction period is 40 min, at $T_{pol} = 40$ °C it is ca. 40 s, and at $T_{pol} = 60$ °C (PA60-566) it is less than 10 s. This induction periods correspond to the pregel reactions when microgels (microparticles richer in BIS than the acrylamide feed) are formed.[30]

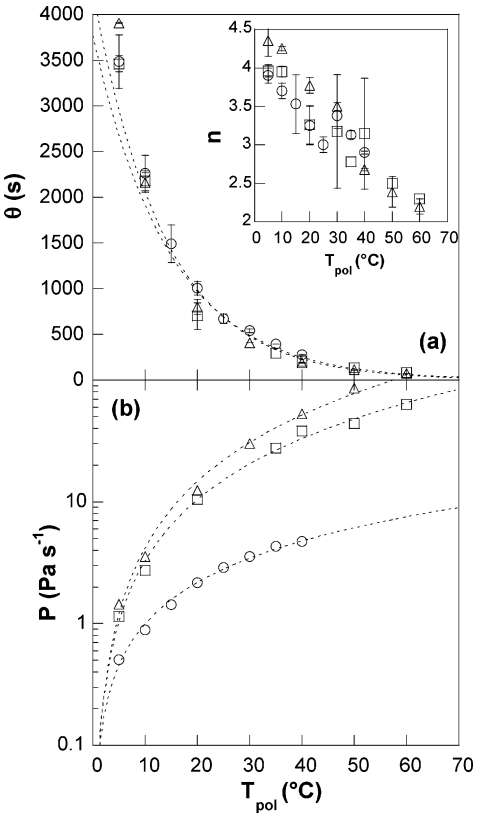

Figure 8. (a) Variation of the half-gelation time θ and exponent n (inset) vs T_{pol} for $\%C = 0.5$ (circles), $\%C = 3.15$ (squares), and $\%C = 5.66$ (triangles). Dotted lines represent the exponential relationship between θ and time. (b) Variation of P (in Pa s^{-1}, calculated from eq 8) plotted vs T_{pol}. Dotted lines are fitted power-law curves.

The characteristic parameters G', θ, and n were extracted from the $G'(t)$ profiles using eq 7. The half-gelation time θ decreases exponentially with T_{pol} (Figure 8a), whereas the coefficient n decreases linearly with T_{pol} (Figure 8a, inset). As expected, the kinetics of the polymerization process strongly depends on T_{pol}. The variation of the asymptotic slope at the half-gelation time P (Figure 8b) shows that the sol−gel transition kinetics increases with T_{pol} and with $\%C$ as described earlier.

In Figure 9, values of steady-state G' (eq 7) are plotted as a function of the polymerization temperature for different $\%C$. There is some difference between the steady-state values of G' measured at T_{pol} and the steady-state values of G' measured after the polymerization at $T = 20$ °C, in regards to the relation $G' = n_e RT$ (eq 9). Steady-state values of G' increases with T_{pol} to reach a maximum value. For $\%C = 0.5$, the maximum gain in elasticity is only ca. 25% obtained from 5 to 25 °C. In contrast, for $\%C = 5.66$ the increase in elasticity reaches 200% from 5 to 50 °C. In general, there is an optimal temperature of polymerization at a given $\%C$ that gives rise to a maximum elasticity. The highest value of G' (14 645 Pa) among all of different conditions is obtained for $T_{pol} = 55$ °C and $\%C = 5.66$.

It is important to note that at high temperature evaporation of hydrogel water can be important even when using a solvent trap. This would result in an increase of G'. This evaporation phenomenon is assumed to be negligible because the gelation was rather fast, i.e. completed within few minutes, and then the temperature was rapidly reduced to 20 °C.

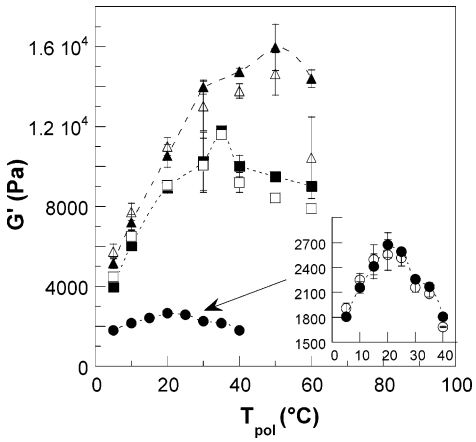

Figure 9. Elastic modulus G' as a function of T_{pol} for $\%C = 0.5$ (circles), $\%C = 3.15$ (squares), and $\%C = 5.66$ (triangles). Closed symbols correspond to G' obtained from eq 7 with $T = T_{pol}$. Open symbols corresponds to G' values measured for $T = 20$ °C (with $\omega = 1$ rad s^{-1} and $\gamma^0 = 0.01$), whatever the T_{pol} used. Inset figure is a blow up of $G'(T_{pol})$ for $\%C = 0.5$.

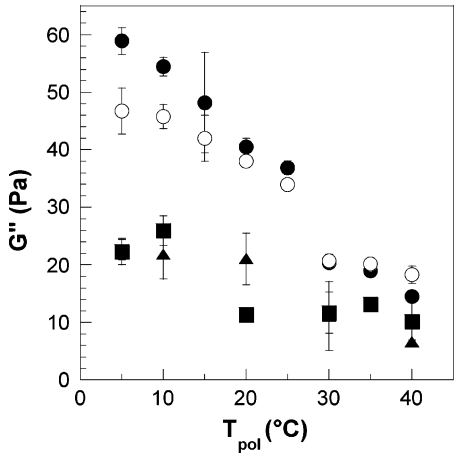

Figure 10. Steady state viscous modulus G'' vs T_{pol} for the three different BIS concentrations polymers used in Figure 9.

The final steady-state viscous moduli G'' were also determined and are presented in Figure 10 as a function of T_{pol} for different $\%C$. For $\%C = 3.15$ and 5.66, G'' is independent of T_{pol} and is ca. 10−20 Pa, which is about 3 orders of magnitude lower than G' values and therefore can be neglected.[21] At $\%C = 0.5$, the hydrogel exhibits some viscous properties; specifically, G'' slightly decreases with T_{pol} and corresponds to ca. 0.9% to 2.5% of the G' values. The viscous modulus G'' is relative to the viscosity of the solvent intrapped within the polymer network.[21] Within a more porous hydrogel, the effective solvent viscosity decreases corresponding to a smaller viscous modulus.

Once the gelation is completed, temperature scanning was performed as previously described. Equations 9 and 10 were used to determine respectively the number of junction n_e and the strand molecular weight M_e as a function of the temperature of polymerization (T_{pol}). Figure 11 shows the linear behavior between G' and the temperature for different T_{pol}. Figure 12 illustrates the variation number of junctions n_e, and the evolution of M_e as a function of T_{pol}. As T_{pol} increases, n_e increases to reach an maximal value. For hydrogels with $\%C = 0.5$, the maximum n_e (1.2 mol m^{-3}) is reached for $T_{pol} = 25$ °C, corresponding to a maximum elasticity of ca. 2700 Pa. For hydrogels with $\%C > 0.5$, the variations of n_e and G' as a function of T_{pol} are similar (Figures 9 and

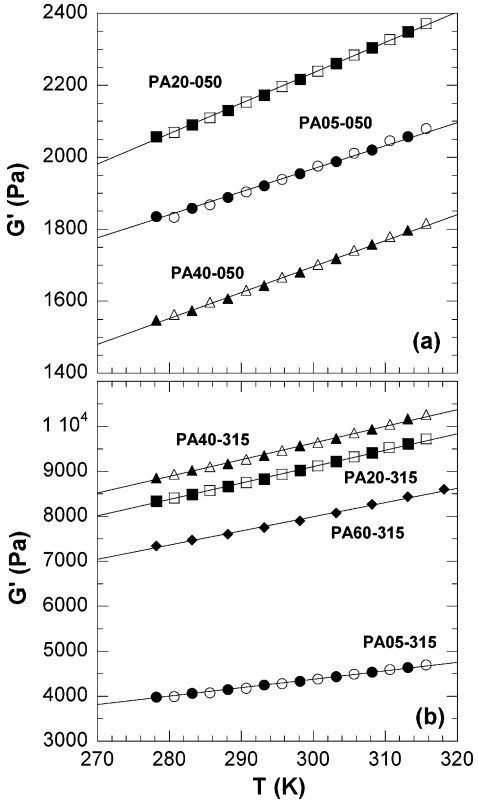

Figure 11. Elastic modulus G' as a function of the temperature (with an equilibrium time of 5 min before measurements using $\omega = 1$ rad s^{-1}, $\gamma^0 = 0.01$) for hydrogels polymerized at different temperatures. Closed symbols represent the heating mode, and open symbol represents the cooling mode. Solid lines represent linear fitting curves.

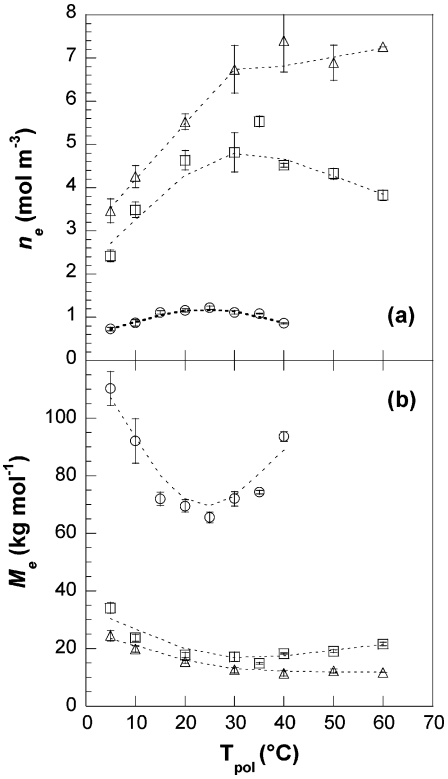

Figure 12. (a) Number of network junctions n_e vs T_{pol} (cf. Figure 11 caption for symbols). Dotted lines are drawn to help interpretation. (b) Strands molecular weights between two junctions M_e as a function of T_{pol}.

12a). The maximum knot density ($n_e \approx 7.2$ mol m^{-3}) is obtained for $\%C = 5.66$ and $T_{pol} \geq 40$ °C. For hydrogels with $\%C = 0.5$, the maximal values of n_e correspond to a minimum molecular weight of the polymer strands M_e ca. 78 kg mol^{-1} (Figure 12b), which suggest short connecting chains. For $\%C = 3.15$ and 5.66, the values of M_e do not vary significantly with $\%C$ but slightly decrease as a function of T_{pol} to finally reach a plateau of ca. 20 kg mol^{-1} at $T_{pol} \approx 20$ °C. For high $\%C$, the values of M_e suggest that connecting chains are about 4 times smaller than with $\%C = 0.5$. A maximum value of elasticity (G' or n_e) is reached at an optimal T_{pol}, which depends on $\%C$. For a constant AAm monomer concentration, this specific optimal T_{pol} increases with increasing $\%C$. Above the optimal temperature, the elasticity decreases and the strand molecular weight increases for $\%C = 0.5$ and 3.15, whereas they are independent of T_{pol} for high cross-link concentration $\%C = 5.66$.

To understand how T_{pol} affects the dissociation of APS initiator and the final network structure of cross-linked PAAm, the elastic modulus G' of cross-linked hydrogels was compared with the viscosity of non-cross-linked PAAm solution synthesized using the same method. Four different T_{pol} were tested (5, 10, 20, and 30 °C). Because of the viscoelastic nature of the polymeric solution obtained, it was more appropriate to perform the polymerization using a cone and plate geometry which provides a uniform shear rate in the gap.[17] When the viscosity of a polymeric solution is larger than at least 4 decades of the solvent viscosity (water viscosity is 0.89 mPa s at 25 °C), one usually concludes that the polymer molecular weight M_w is larger than the critical molecular weight M_c for which entanglements between the polymer chains become important. For PAAm in water at 25 °C, M_c was estimated to be ca. 4.4×10^5 g mol^{-1}.[41] Then, the zero-shear viscosity is related to the molecular weight by[41,42]

$$\eta_0 = KM_w^{3.4} \tag{11}$$

where K is a constant relative to the polymer/solvent pair.

Once complete polymerization was achieved, the shear flow viscosities $\eta(\dot{\gamma})$ vs the shear rate $\dot{\gamma}$ were recorded at 20 °C (Figure 13). The zero-shear viscosities η_0 were estimated using the Carreau−Yasuda model law[43,44] and plotted as a function of T_{pol} (Figure 13, inset). η_0 exponentially decreases as T_{pol} increases according to the following relation:

$$\eta_0 = 6128e^{-0.16T_{pol}} \tag{12}$$

The molecular weight decreases with increasing the temperature of polymerization according to $M_w^{3.4} = K'e^{-0.16T_{pol}}$. As the initial monomer concentration is constant (8% w/v), the exponential decreases of η_0 and M_w with T_{pol} are due to an increase in active initiator concentration in the solution, leading to the synthesis of shorter but a higher number of polymer chains. It is known that for acrylamide polymerization the kinetic constant of the propagation reaction is considerably larger than the kinetic constants of APS dissociation and ending reactions.[45,46] The dissociation of APS in radicals is the most temperature-sensitive step in the reaction.[32] For the cross-linked hydrogel, it is conceivable that increasing T_{pol} would favor the activation of

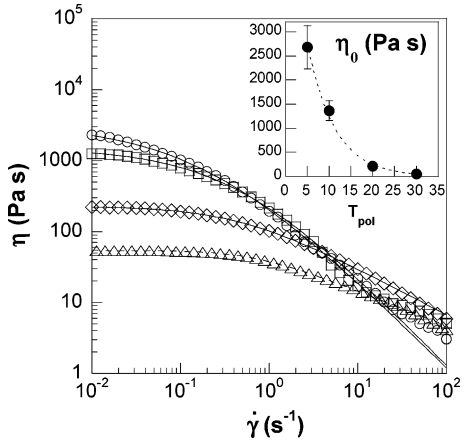

Figure 13. Main graphic: shear viscosity $\eta(\dot{\gamma})$ measured at 20 °C for un-cross-linked PAAm hydrogels (8% w/v) synthesized at temperatures of 5 °C (circles), 10 °C (squares), 20 °C (diamonds), and 30 °C (triangles). The solid lines represent the fitted curves using the Carreau−Yasuka model.[44] Inset: zero-shear viscosity estimated from the fit of $\eta(\dot{\gamma})$ as a function of polymerization temperature (T_{pol}). Dotted line represents an exponential curve fit.

initiators during the initiation period, which in turn promote the formation of more junction knots (between AAm and BIS monomers, i.e., formation of more microgels) and shorter strands, leading to higher elasticity. The decrease of G' (and n_e) as T_{pol} increases can be explained by the fact that at high polymerization temperature the maximum potential junctions (microgels) are formed during the initiation period, and then fewer AAm monomers are available to link the microgels during the sol−gel transition, for the same concentration in acrylamide monomer (8 wt %). The microgels are present in the solution, but they are not elastically active because of the lack of the number of active strands. Indeed, Tanaka[25] and Peckan et al.[11] have observed, using light scattering technique, an increased in the number of clusters in the gel as T_{pol} increases. Rheological data (decrease of G' as a function of T_{pol}) suggest that some clusters are not linked to three or more active strands or remain free in the hydrogel and therefore are not elastically active.

The increase of $\%C$ at constant T_{pol}, or the increase of T_{pol} at constant $\%C$, leads to the formation of more microgels which can act as potential active junctions and larger strands (G' increases) until it reaches an optimal value, followed by a decrease (in G') due to the fact that the monomer concentration is constant.

4. Conclusion

To better understand the formation and the final structure of PAAm hydrogels, the influence of the cross-linker concentration and the polymerization temperature during the polymerization process was studied using rheological monitoring. Generally, the structure (mesh size) is changed by modulating the molar ratio of the monomer and the cross-linker. In this study, BIS concentration and polymerization temperature were varied to determine the optimal synthesis condition for attaining the maximum elasticity for a given AAm concentration. Rheological monitoring of the syntheses was performed using small dynamic oscillatory deformations. The rheological properties of the hydrogels are mainly represented by the elastic modulus G' and described by the rubber elasticity theory $G' = n_eRT$, where n_e is the number of effective junctions in the polymeric network. An increase in the amount of cross-linker in the hydrogel leads to a linear increase of the steady state G'. However, above a threshold cross-linker concentration ($\%C = 4.2$ for global concentration of monomer of 8% w/v), the elasticity reaches a maximal value. We demonstrated that the polymerization temperature strongly influences the reaction kinetics and also the final elastic modulus for cross-linked hydrogels or the zero-shear viscosity for un-cross-linked hydrogel.

For all of the cross-linked hydrogels synthesized, the number n_e was also determined from a temperature scan of the steady-state elastic modulus. $G'(T)$ increases linearly, allowing the direct determination of n_e using the equation $G' = n_eRT$. Steady state G' and n_e have the same behavior as a function of the cross-linker concentration ($\%C$) or the polymerization temperature (T_{pol}).

The results were explained on the basis of the fact that increasing temperature affects the dissociation of the initiator into radicals. To confirm this point, linear un-cross-linked PAAm were synthesized with the same acrylamide concentration but at different T_{pol}. Zero-shear viscosities, η_0, and then the molecular weights, M_w, exponentially decrease in function of T_{pol}. As T_{pol} controls the number and the weight of linear PAAm chains synthesized, T_{pol} also controls the number of junctions and active strands in cross-linked PAAm in the hydrogels. The decrease in elasticity as the temperature is further increased is explained by the lack of AAm monomers to elastically engage all of the junctions present in the solution.

The study demonstrated that, for a fixed acrylamide monomer concentration, there is a unique gelation temperature for a specific cross-linker concentration that gives the maximum elasticity. Rheological monitoring during hydrogel synthesis is therefore a powerful tool to determine the best polymerization conditions leading to the desired structure and properties.

Acknowledgment. This work was supported by the Natural Sciences and Engineering Research Council of Canada (NSERC) and the Centre de Recherche en Sciences et Ingénierie de Macromolécules (CERSIM, Québec, Canada). J. Y. Wong acknowledges support from NIH R01 HL72900-01A1. The authors thank Pr Pierre Carreau (Ecole polytechnique, Montreal) and Pr Julian Zhu (Chemistry Department, University of Montreal) for valuable discussions and rheological measurements.

References and Notes

(1) Cohen, Y.; Ramon, O.; Kopelman, I. J.; Mizrahi, S. *J. Polym. Sci., Part B: Polym. Phys.* **1992**, *30*, 1055−1067.
(2) Hecht, A. M.; Duplessix, R.; Geissler, E. *Macromolecules* **1985**, *18*, 2167−2173.
(3) Kara, S.; Pekcan, O. *J. Appl. Polym. Sci.* **2001**, *80*, 823−830.
(4) Ferreira, L.; Vidal, M. M.; Gil, M. H. *Chem. Educ.* **2001**, *6*, 100−103.
(5) Wang, Y. L.; Pelham, R. J. *Mol. Mot. Cytoskeleton, Part B* **1998**, *298*, 489−496.
(6) Wong, J. Y.; Velasco, A.; Rajagopalan, P.; Pham, Q. *Langmuir* **2003**, *19*, 1908−1913.
(7) Hoffman, A. S. *Adv. Drug Delivery Rev.* **2002**, *54*, 3−12.
(8) Anseth, K. S.; Bowman, C. N.; BrannonPeppas, L. *Biomaterials* **1996**, *17*, 1647−1657.
(9) Baselga, J.; Hernandez-Fuentes, I.; Pierola, I. F.; Llorente, M. A. *Macromolecules* **1987**, *20*, 3060−3065.
(10) Mallam, S.; Horkay, F.; Hecht, A. M.; Geissler, E. *Macromolecules* **1989**, *22*, 3356−3361.

(11) Pekcan, O.; Kara, S. *Polym. Int.* **2003**, *52*, 676−684.
(12) Durmaz, S.; Okay, O. *Polym. Bull. (Berlin)* **2001**, *46*, 409−418.
(13) Crescenzi, V.; Dentini, M.; Bontempo, D.; Masci, G. *Macromol. Chem. Phys.* **2002**, *203*, 1285−1291.
(14) Grattoni, C. A.; Al-Sharji, H. H.; Yang, C. H.; Muggeridge, A. H.; Zimmerman, R. W. *J. Colloid Interface Sci.* **2001**, *240*, 601−607.
(15) Winter, H. H.; Chambon, F. *J. Rheol.* **1886**, *30*, 367−382.
(16) Weiss, N.; Silberberg, A. *Br. Polym. J.* **1977**, *June*, 144−150.
(17) Macosko, C. W. *RHEOLOGY Principles, Measurements, and Applications*; Wiley-VCH: New York, 1994.
(18) Flory, P. J. *J. Am. Chem. Soc.* **1941**, *63*, 3083−3090, 3091−3096, 3096−3100.
(19) Flory, P. J. *Principles of Polymer Chemistry*; Cornell University Press: Ithaca, NY, 1953.
(20) Ferry, J. D. *Viscoelastic Properties of Polymers*, 3rd ed.; Wiley: New York, 1980.
(21) Kulicke, W. M.; Nottelmann, H. *Adv. Chem. Ser.* **1989**, 15−44.
(22) Benguigui, L. *J. Phys. II* **1995**, *5*, 437−443.
(23) Benguigui, L.; Boue, F. *Eur. Phys. J. B* **1999**, *11*, 439−444.
(24) Gelfi, C.; Righetti, P. G. *Electrophoresis* **1981**, *2*, 220−228.
(25) Takata, S.; Norisuye, T.; Shibayama, M. *Macromolecules* **1999**, *32*, 3989−3993.
(26) Matsuo, E. S.; Orkisz, M.; Sun, S. T.; Li, Y.; Tanaka, T. *Macromolecules* **1994**, *27*, 6791−6796.
(27) Riihimaki, T. A.; Middleman, S. *Macromolecules* **1974**, *7*, 675−680.
(28) Patras, G.; Qiao, G. G.; Solomon, D. H. *Macromolecules* **2001**, *34*, 6396−6401.
(29) Trompette, J. L.; Fabregue, E.; Cassanas, G. *J. Polym. Sci., Part B: Polym. Phys.* **1997**, *35*, 2535−2541.
(30) Baselga, J.; Llorente, M. A.; Hernandezfuentes, I.; Pierola, I. F. *Eur. Polym. J.* **1989**, *25*, 477−480.
(31) Pekcan, O.; Kara, S. *Polymer* **2001**, *42*, 10045−10053.
(32) Hames, B. D. In *Gel Electrophoresis of Proteins: A Practical Approach*, 2nd ed.; Rickwood, B. D. H. A. D., Ed.; Oxford University Press: New York, 1990; pp 1−149.
(33) Kizilay, M. Y.; Okay, O. *Polymer* **2003**, *44*, 5239−5250.
(34) Giraldo, J.; Vivas, N. M.; Vila, E.; Badia, A. *Pharmacol. Therap.* **2002**, *95*, 21−45.
(35) Hill, A. V. *Biochem. J.* **1913**, *7*, 471−480.
(36) Naghash, H. J.; Okay, O. *J. Appl. Polym. Sci.* **1996**, *60*, 971−979.
(37) Baselga, J.; Llorente, M. A.; Hernandezfuentes, I.; Pierola, I. F. *Eur. Polym. J.* **1989**, *25*, 471−475.
(38) Ferry, J. D. *Viscoelastic Properties of Polymers*, 3rd ed.; John Wiley & Sons: New York, 1980.
(39) Atkins, P. W. *Physical-Chemistry*, 6th ed.; Freeman: New York, 1998.
(40) Giz, A.; Catalgil-Giz, H.; Alb, A.; Brousseau, J. L.; Reed, W. F. *Macromolecules* **2001**, *34*, 1180−1191.
(41) Kulicke, W. M.; Kniewske, R.; Klein, J. *Prog. Polym. Sci.* **1982**, *8*, 373−468.
(42) Grigorescu, G.; Kulicke, W. M. *Adv. Polym. Sci.* **2000**, *152*, 1−40.
(43) Carreau, P. J. *J. Rheol.* **1972**, *16*, 99−127.
(44) Ortiz, M.; De Kee, D.; Carreau, P. J. *J. Rheol.* **1994**, *38*, 519−539.
(45) Pascal, P.; Napper, D. H.; Gilbert, R. G.; Piton, M. C.; Winnik, M. A. *Macromolecules* **1990**, *23*, 5161−5163.
(46) Pascal, P.; Winnik, M. A.; Napper, D. H.; Gilbert, R. G. *Macromolecules* **1993**, *26*, 4572−4576.

MA049072R